AN INVESTIGATION OF THREE MAJOR TIME-SERIES DATA ANALYSIS TECHNIQUES

J. R. Red-Horse[1], K. F. Alvin[1], M. P. Mignolet[2], A. N. Robertson[3]

[1]P.O. Box 5800, Mail Stop 0439
Sandia National Laboratories
Albuquerque, NM 87185

[2]Dept of Aerospace and Mechanical Engineering
Arizona State University
Tempe, AZ 85287-6106

[3]Center for Aerospace Structures (CAS)
University of Colorado at Boulder
Campus Box 429
Boulder, Colorado 80309-0429

1 Abstract

In this article, a study comparing three time series data analysis techniques is undertaken. These techniques include a traditional spectral approach, wavelet transforms, and autoregressive with exogenous input. The study is motivated by the current popularity of discrete-time data reduction schemes, such as the Eigensystem Realization Algorithm and Polyreference, for extracting test-derived modal models from measurement data in the modal testing community and problems associated with acquiring the input to them via intermediate approximations to continuous-time system characterizations. A review of pertinent details for each of the approaches is given and all are compared through results of a computational example.

2 Nomenclature

$\mathbf{A}, \mathbf{B}, \mathbf{C}, \mathbf{D}$	: Continuous-Time State Matrices
$\mathbf{x}(t)$	: State Vector
$\mathbf{u}(t)$	: Input (Excitation) Vector
$\mathbf{y}(t)$	: Output (Response) Vector
$\mathbf{h}(t)$	: Continuous-Time Impulse Response
$\bar{\mathbf{A}}, \bar{\mathbf{B}}$	: Discrete-Time State Matrices
$\bar{\mathbf{h}}(i)$	: Discrete-Time Impulse Response
$R_{uu}(\tau)$	: Input Autocorrelation Function
$R_{yy}(\tau)$	: Output Autocorrelation Function
$R_{yu}(\tau)$	: Input/Output Cross-correlation Function
$S_{(\cdot\cdot)}(\omega)$	: Power Spectral Density Function
$\mathbf{H}(\omega)$	: Frequency Response Matrix
$\mathbf{Y}$	: Output Matrix
$\mathbf{U}$	: Input Matrix
$[\cdot]^{DWT}$	: Denotes Discrete Wavelet Transform
A_i, B_i, C_0	: ARX Coefficient Matrices
δ_{kl}	: Kronecker Delta Symbol

3 Introduction

Structural dynamics test model characterization may be effected in a number of ways depending on the specifications for and constraints placed upon a given modal test [1]. By far the most popular approach culminates in the derivation of a modal model from sampled time-domain response measurements obtained for a set of degrees of freedom (DOF) on the physical structure under consideration. Such models are often used subsequently as vital elements of an overall structural design strategy for such purposes as establishing a physically-validated data point for updating analytically derived models.

Because of the discretized nature of the response measurements used, modal models are often derived from data in a discrete, sampled-data form. Many of the more recent approaches for reducing measurement data to modal models, such as Polyreference [2] and ERA [3], are based on discrete time domain input/output characterizations and require an estimate of the discrete-time impulse response functions for each input/output pairing. Often called Markov parameters in the literature, the points that make up the discrete impulse response represent fundamental properties of the sampled–data model which is itself derived from the continuous-time equations of motion for the structure given a sampling rate and assumptions regarding the variation of the input between samples. The present study focuses on methods for estimating the desired discrete impulse response from the general input and output time series measurements available in modal testing.

The current state-of-the-art for obtaining the discrete impulse response functions from the set of response measurements comprises what is known collectively as *spectral methods*. Spectral methods involve computing multiple-input/multiple-output (MIMO) frequency response functions (FRF) from discrete Fourier transforms of the input and output time signals. Their use became widely popular with the advent of the Fast Fourier transform (FFT) algorithm. Although the FFT facilitated modal testing through its computational speed and the ease with which the algorithm can be implemented in the data acquisition hardware,

there are a number of additional advantages that make spectral methods popular. Among these are the ability to perform what is, in essence, a preliminary data reduction by averaging the FFT'd data in the frequency domain—although the actual averaging is most often performed on the auto and cross spectral density function estimators. Storing the running frequency domain averages, as opposed to a collection of time history data, results in a significant memory savings. And, while it's more natural to think of spectral approaches in the context of random data, the method lends itself quite well to the deterministic framework where the resulting FRF's can be interpreted as least squares, equivalent linear models fit to the data.

Even with all the advantages inherent to spectral methods, there are relevant drawbacks to consider. The signals undergo the well-known corruptive influences of leakage and aliasing; and, while mitigation procedures for these phenomena are also well-known, the associated side effects are often nontrivial. A more fundamental issue pertains to the conflicting requirements that the signals be limited both in time duration and frequency bandwidth. Finally, given an ultimate goal of deriving accurate estimate of the discrete impulse functions, it is important to consider their relationship to the discrete FRFs through the use of the discrete Fourier transform, and the relationship between the continuous and discrete FRF's. For example, in lightly damped systems, there can be significant errors introduced in the computation of the discrete impulse response due to the frequency resolution of the FRF. In addition, the discrete and continuous FRFs can differ remarkably in both magnitude and phase, particularly away from the resonance peaks, because of the implicit ambiguity in the variation of the signals between samples. Thus, severe limitations are posed by use of spectral methods for discrete impulse response estimation, even when the continuous FRFs are estimated to the highest levels of accuracy.

It is this latter issue that motivates the current study in which we explore two additional data reduction approaches, Autoregressive with eXogenous input (ARX) and Wavelet Transforms, for estimating system Markov parameters which represents the data necessary for subsequent input to time domain-based modal model algorithms. Both of these approaches are particularly relevant to the aforementioned issues because they seek to bypass the corrupting effects of the discrete forward and inverse Fourier transforms by estimating the Markov parameters in the time domain using a discrete time input/output system characterization consistent with the model form used in the subsequent modal model derivation. The ARX method has been studied and used extensively for modal model derivation. In the present context, it is used in a systematic way to determine an over-parameterized input/output model, which in turn is used to compute the impulse responses. The wavelet transform-based technique, on the other hand, attempts to estimate the impulse responses through a discrete deconvolution of the data represented in terms of wavelet transform coefficients.

4 Overview of The Methods

In this section, an overview of the salient features of each of the techniques is presented. The reader is directed to the cited references for more detailed discussions associated with any of the approaches.

All methods for data fitting begin by inferring an underlying model form and the data are then collected and fit to parameters of that model. For the methods currently under consideration, a linear relationship is presumed, viz.,

$$\begin{aligned} \dot{\mathbf{x}}(t) &= \mathbf{A}\mathbf{x}(t) + \mathbf{B}\mathbf{u}(t) \\ \mathbf{y}(t) &= \mathbf{C}\mathbf{x}(t) + \mathbf{D}\mathbf{u}(t) \end{aligned} \tag{1}$$

The output $\mathbf{y}$ and input $\mathbf{u}$ are then related through a convolution integral:

$$\begin{aligned} \mathbf{y}(t_n) &= \int_{-\infty}^{t_n} \mathbf{h}(t_n - \tau)\mathbf{u}(\tau)d\tau \\ &= \int_0^1 \mathbf{h}(\theta)\mathbf{u}(t_n - \theta)d\theta \end{aligned} \tag{2}$$

where $\mathbf{h}(\theta)$ is the temporal impulse response function of (1).

For a discrete-time system of the corresponding state space form

$$\begin{aligned} \mathbf{x}(i+1) &= \bar{\mathbf{A}}\mathbf{x}(i) + \bar{\mathbf{B}}\mathbf{u}(i) \\ \mathbf{y}(i) &= \mathbf{C}\mathbf{x}(i) + \mathbf{D}\mathbf{u}(i) \end{aligned} \tag{3}$$

the convolution integral is transformed to a summation involving samples of the input, $\mathbf{u}(i)$ and the discrete-time impulse response function, $\bar{\mathbf{h}}(i)$

$$\mathbf{y}(n) = \sum_{k=0}^{n} \bar{\mathbf{h}}(n-k)\mathbf{u}(k) \tag{4}$$

The Markov parameters, $\bar{\mathbf{h}}(i)$, are related analytically to their continuous-time counterpart, $\mathbf{h}(\theta)$, via integration over the time step, Δt, of the discrete-time system along with some assumptions regarding the variation of the input between the samples.

There is an important theoretical issue underlying discrete impulse response estimation for continuous systems; that is, the differences between the continuous and discrete frequency response and the corresponding differences in the impulse response functions. Figure 1

illustrates these differences for a simple four degree-of-freedom system with force input and acceleration output. The continuous FRF results from sampling the transfer function

$$\mathbf{H}(s) = \mathbf{D} + \mathbf{C}(s\mathbf{I} - \mathbf{A})^{-1}\mathbf{B} \tag{5}$$

of the continuous system (1) at $s = j\omega$ for a discrete set of N frequencies ω_k. The discrete FRF at the same frequencies ω_k is generated by computing the impulse response of the system discretized with a zero-order hold, given by

$$\begin{aligned} \bar{\mathbf{h}}(0) &= \mathbf{D} \\ \bar{\mathbf{h}}(i) &= \mathbf{C}\bar{\mathbf{A}}^{i-1}\bar{\mathbf{B}} \qquad i = 1, \ldots N-1 \end{aligned} \tag{6}$$

where

$$\bar{\mathbf{A}} = e^{\mathbf{A}\Delta t} \qquad \bar{\mathbf{B}} = \int_0^{\Delta t} e^{\mathbf{A}(\Delta t - \tau)}\mathbf{B}\, d\tau \tag{7}$$

and then taking the discrete Fourier transform of $\bar{\mathbf{h}}$ to obtain the discrete FRF, $\bar{\mathbf{H}}(j\omega)$. The differences

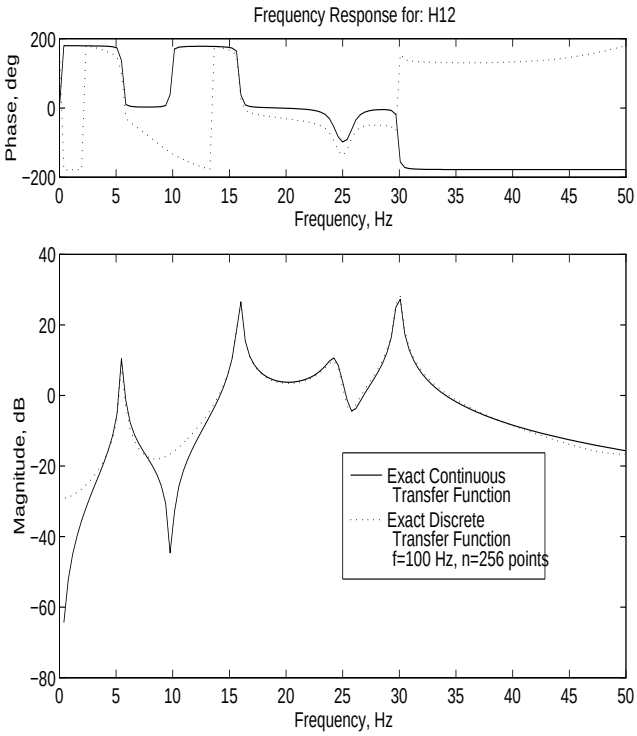

Figure 1: Comparison of Continuous and Discrete Frequency Response Functions

between the two FRFs, both of which are "exact" in the sense that they are computed directly from the equations of motion, are due both to sampling and to windowing effects. The sampling causes aliasing of responses above the Nyquist frequency (half of the sampling frequency), which in this case is due to the high frequency asymptote of the acceleration response coupled with the high frequency input of the zero-order hold. This affects primarily the lower magnitude responses, such as those near the transmission zeros of the continuous FRF.

Although at first it might seem that the discrete FRF is inferior to the continuous FRF in terms of characterizing the dynamics of the system, given that it is distorted by aliasing and windowing, it is actually this FRF which proves the more desirable alternative. This is the case since, for subsequent modal model identification using approaches such as ERA or Polyreference, the estimated FRF must be transformed to the time domain using an inverse discrete Fourier transform. For the discrete FRF, this final step can be viewed as reversing the distortions caused by aliasing and windowing in such a way that the resultant impulse response is identical to that used to create the discrete FRF, and is the exact discrete impulse response of the system. The inverse discrete Fourier transform of the exact continuous FRF is also prone to a reversal of aliasing and windowing effects, but in this case the distortion is not balanced by the forward transform resulting in a discrete impulse response which is not equivalent to the exact Markov parameters of the discretized system.

In summary, before proceeding to a detailed discussion of the estimation algorithms, we wish to point out that the system can be characterized by either continuous or discrete response functions, and that those functions are not merely samples or interpolations of each other. They in fact can be quite different and reflect the limitations of discrete transforms and models as applied to continuous systems.

4.1 Spectral Methods

Consider equation (2) and assume that the input term is a random vector process, then multiplying both sides of the equation by $\mathbf{u}(t-\tau)^T$ and taking mathematical expectation of both sides of the resulting equation yields

$$R_{yu}(\tau) = \int_{-\infty}^{\infty} \mathbf{H}(\theta) R_{uu}(\tau - \theta)\, d\theta \tag{8}$$

which, upon taking the Fourier transform, results in the following relationship:

$$S_{yu}(\omega) = \mathbf{H}(\omega) S_{uu}(\omega) \tag{9}$$

where $R_{(\cdot\cdot)}(\tau)$ are the auto and cross correlation functions and $S_{(\cdot\cdot)}(\omega)$ are the auto and cross spectral density functions.

Alternatively, one could replace $\mathbf{u}(t-\tau)^T$ with $\mathbf{y}(t-\tau)^T$ and follow a similar path to

$$S_{yy}(\omega) = \mathbf{H}(\omega) S_{uy}(\omega) \tag{10}$$

Thus the frequency response, $\mathbf{H}$, can be estimated from either of equations (9) or (10). and the respective quantities are commonly referred to as $\mathbf{H}_1$ and $\mathbf{H}_2$. Each estimate can give rise to different results and the applicability of each in the face of various noise models is generally addressed in the literature on modal testing (e.g. [1]).

Given the above theory, one is left with the task of *estimating* these continuous spectra using finite, sampled time history data; and, if one considers the derivation of the discrete system Markov parameters as the ultimate goal, this is where the complicating factors begin to surface. Among them are:

- FFTs of finite length sampled time data records impose an assumed periodicity in both the time and frequency domain representations. One consequence of this is a phenomenon known as leakage, which results when frequency components of the signal are not integer multiples of the discrete frequency resolution, Δf.
- All continuous structures contain, at a minimum, a countably infinite eigenvalue spectrum, which translates into the existence of modes above the cutoff frequency for the sampled data. Furthermore, when acceleration sensors are utilized, the transfer functions of the system modes, including those below the cutoff frequency, possess a high frequency, nonzero, asymptote. Those out-of-band response components are aliased down into the frequency band of interest unless some care is made in designing the excitation and in acquiring the data.

4.2 Wavelet Transforms

Wavelet transforms provide a new methodology for estimating the Markov parameters of MIMO dynamic systems [4]. As with the spectral approach, the method involves transforming the time domain convolution integral, although with wavelets the result is a new convolution problem written in terms of the wavelet transform coefficients. Hence, the wavelet-based approach is more closely related to a classical time domain deconvolution, whereby the Markov parameters are estimated through a numerical inversion of the discrete-time convolution equations. Both the wavelet and time domain approaches yield similar solutions, but additional improvements are possible when done in the wavelet domain due to the unique filtering properties of the wavelet transform.

The discretized convolution given in equation (4) can be expressed in matrix form as:

$$\mathbf{Y} = \mathbf{hU} \tag{11}$$

where the output matrix $\mathbf{Y}$, the time-domain impulse response matrix $\mathbf{h}$ and the input matrix $\mathbf{U}$ are given, respectively, by

$$\mathbf{Y}_{[m\times s]} = \left\{ \begin{array}{cccc} \mathbf{y}(0) & \mathbf{y}(1) & \ldots & \mathbf{y}(s-1) \end{array} \right\} \tag{12a}$$

$$\mathbf{h}_{[m\times r(p+1)]} = \left\{ \begin{array}{cccc} \mathbf{h}(0) & \mathbf{h}(1) & \ldots & \mathbf{h}(p) \end{array} \right\} \tag{12b}$$

$$\mathbf{U}_{[r(p+1)\times s]} = \left[\begin{array}{ccccc} \mathbf{u}(0) & \cdots & \mathbf{u}(p) & \cdots & \mathbf{u}(s-1) \\ 0 & \ddots & \vdots & \ddots & \vdots \\ 0 & 0 & \mathbf{u}(0) & \cdots & \mathbf{u}(s-p-1) \end{array} \right] \tag{12c}$$

The subscripts on the left-hand sides of the above equations represent the matrix sizes for which m, s, r and p are the number of measurement vectors, the number of measurement samples, the number of input signals, and the number of discrete impulse response parameters, respectively. The parameter p depends of the decay rate of the impulse response; for structures with light damping $p = s - 1$ since it cannot be assumed that $h(p) = 0$ for $p < s - 1$.

Equation (4) can thus be represented in the wavelet domain by taking the discrete wavelet transforms (DWT) of both $\mathbf{h}$ and $\mathbf{u}$:

$$\mathbf{h}^{DWT}(\theta) = h_0^{DWT} + \sum_j \sum_k h_{(2^j+k)}^{DWT} \psi(2^j\theta - k) \tag{13}$$

For the DWT characterization of $\mathbf{u}(t_n - \theta)$, first $\mathbf{u}(\theta)$ is reversed in time to obtain $\mathbf{u}(-\theta)$, then it is shifted toward the positive time axis by the amount t_n and $\{\mathbf{u}(\theta) = 0, \quad \text{for} \quad \theta > t_n\}$. With this convention, the DWT series of $\mathbf{u}(t_n - \theta)$ is expressed as:

$$\mathbf{u}^{DWT}(t_n - \theta) = u_0^{DWT} + \sum_j \sum_k u_{(2^j+k)}^{DWT} \psi(2^j\theta - k) \tag{14}$$

Substituting the DWT series of $\mathbf{h}^{DWT}(\theta)$ and $\mathbf{u}^{DWT}(t_n - \theta)$ into the above convolution integral for $\mathbf{y}(t_n)$, while utilizing wavelet orthogonality conditions [5], one obtains the following formula [6]:

$$\mathbf{y}(t_n) = \mathbf{h}^{DWT}\mathbf{u}^{DWT}(t_n) \tag{15a}$$

$$\mathbf{h}^{DWT} = \begin{array}{cccccccc} h_0 & h_1 & h_2 & h_3 & h_4 & h_5 & \ldots \end{array} \tag{15b}$$

$$\mathbf{u}^{DWT^T} = \begin{array}{cccccc} u_0 & u_1 & u_2/2 & u_3/2 & \ldots \end{array} \tag{15c}$$

where $\mathbf{h}^{DWT}$ is the wavelet transform of $\mathbf{h}(\theta)$ and $\mathbf{u}^{DWT}(t_n)$ is the wavelet transform of $\{\mathbf{u}(t_n - \theta), \quad 0 \leq \theta \leq t_n\}$.

For the entire response data, one can arrange the input and output relation in the form

$$\underset{[m\times s]}{\mathbf{Y}} = \underset{[m\times r\ell]}{\mathbf{h}^{DWT}} \quad \underset{[r\ell\times s]}{\mathbf{U}^{DWT}} \tag{16}$$

where

$$\mathbf{Y} = \{\mathbf{y}(0),\ \ \mathbf{y}(1),\ \ \ldots\} \tag{17a}$$

$$\mathbf{U}^{DWT} = \{\mathbf{u}^{DWT}(0),\ \mathbf{u}^{DWT}(1),\ \ldots\} \tag{17b}$$

and m, s, r and ℓ are the number of measurement vectors, the number of measurement samples, the number of input signals, and the depth of the wavelet transform levels, respectively. Note, this is in the same form as the time domain problem (2), except that the $\mathbf{h}$ and $\mathbf{U}$ matrices are transformed to the wavelet domain.

Solving for $\mathbf{h}^{DWT}$ from the above relation, one obtains

$$\mathbf{h}^{DWT} = \mathbf{Y} \cdot \mathbf{U}^{DWT^T} \cdot \left(\mathbf{U}^{DWT}\mathbf{U}^{DWT^T}\right)^{-1} \tag{18}$$

and finally the inverse DWT of $\mathbf{h}^{DWT}$ yields the desired temporal impulse response data:

$$\{\mathbf{h}(t),\quad t = t_0,\ t_1, \ldots, t_{(s-1)}\} = IDWT\{\mathbf{h}^{DWT}\}. \tag{19}$$

For systems with multiple inputs, it is necessary to use multiple test data batches to obtain a well-conditioned solution. In this case, the quantities $\mathbf{U}^{DWT}\mathbf{U}^{DWT^T}$ and $\mathbf{Y} \cdot \mathbf{U}^{DWT^T}$ are averaged over an ensemble of test data. This averaging approach is also helpful in handling measurement noise.

4.3 Exogenous Autoregressive (ARX) Modeling

Contrary to traditional spectral analysis and the wavelet transform technique described above, the exogenous autoregressive (ARX) modeling approach is based on a different parametric representation of the system's input/output relationship. Specifically, it is assumed that the input sequence, $\mathbf{u}(n)$, n=0,1,2,... and the corresponding output, $\mathbf{y}(n)$, satisfy the recurrence equation specified by

$$\begin{aligned}\mathbf{y}(n) + A_1\mathbf{y}(n-1) + \ldots + A_p\mathbf{y}(n-p) = \\ B_0\mathbf{u}(n) + \ldots + B_q\mathbf{u}(n-q) + C_0\mathbf{w}(n)\end{aligned} \tag{20}$$

where the coefficients A_i, i=1, 2, ..., p, B_j, j=0,1, 2, ..., q, and C_0 are constant matrices and $\mathbf{w}(n)$ denotes a uncorrelated Gaussian white noise vector.

ARX models (see [7] and references therein for additional details) can be shown to be a special case of a more general class, known as exogenous autoregressive moving average (ARMAX) models, which have been found to represent the input/output relationship of multi-degree-of-freedom dynamic systems (see, for example, [8, 9, 10]) under very broad conditions.

Given samples of the input $\mathbf{u}(n)$ and output $\mathbf{y}(n)$ time series, determination of the parameters, A_i, B_j, and C_0, proceeds following standard arguments [7]: The coefficients are evaluated through maximization of a likelihood function based on the observed response time series or, equivalently, the minimization of an error metric, ε_L, defined by

$$\varepsilon_L = \sum_n \left[\sum_{i=0}^{p} A_i\ \mathbf{y}(n-i)\ -\ \sum_{j=0}^{q} B_j\ \mathbf{u}(n-j)\right]^2 \tag{21}$$

where A_0 is constrained to be the identity matrix. Note that ε_L is quadratic in the unknown elements of the matrices A_i, i=1, 2, ..., p, B_j, j=0,1, 2, ..., q so that these coefficients can be obtained by solving a linear system of equations.

Once the ARX model coefficients have been determined, the frequency response function of the system can directly be estimated in the form

$$\mathbf{H}(\omega) = \left[\sum_{k=1}^{p} A_k\ e^{-ik\omega\Delta T}\right]^{-1} \left[\sum_{l=1}^{q} B_l\ e^{-il\omega\Delta T}\right] \tag{22}$$

where ΔT denotes the sampling time.

Alternatively, the Markov parameters of the system can recursively be estimated from Eq. (1) with the input sequence

$$\mathbf{u}(n) = \begin{bmatrix} 1 & 0 & 0 & \\ 0 & 1 & 0 & \cdots \\ 0 & 0 & 1 & \\ & \vdots & & \ddots \end{bmatrix} \delta_{n0} \tag{23}$$

where δ_{kl} denotes the Kronecker symbol.

5 Example Applications

In this section, we attempt to examine the similarities and differences exhibited by the methods via numerically simulated example situations for a four degree system. This system, which is shown graphically in Figure 2, consists of four masses connected to each other, and to one rigid reference location, via springs and viscous damping elements. These discrete DOF are numbered as shown with excitations applied at DOF 2 and 4. For all of the cases considered we assume a sample rate of 100Hz, which corresponds to $\Delta t = .01$ seconds, and show results for a subset of the estimated data. Specifically, frequency response functions for the response at DOF 1 due to excitation at DOF 2 will be given.

The simulation of the system was carried out as follows. In the first example, discrete random excitation signals were generated at $1000Hz$ to approximate stationary

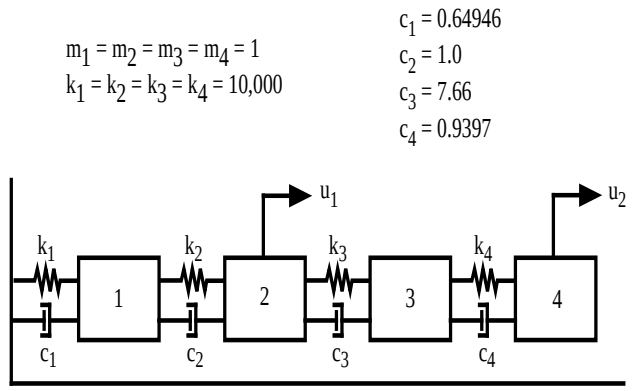

Figure 2: Sketch of Four DOF System

Gaussian white noise. These signals were low-pass filtered at $50Hz$ and applied to the continuous equations of motion with a first-order hold to approximate the application of an analog input signal to the structure. The inputs and outputs were then computed at intervals of 0.001 seconds. Finally, these "continuous" signals were contaminated with one percent measurement noise and then sampled to $100Hz$ to obtain the final digital signals used for response function estimation. A total of 10240 samples were obtained, corresponding to a 102.4 second duration simulated test.

For averaging purposes, in the case of the FFT-based spectral estimation and the Wavelet transform method, the data records were finally partitioned into an ensemble of 40 records, each containing 256 samples for each input and output signal. The results for all three methods are shown in Figure 3. Note that both the wavelet transform (albeit with slight problems at the extreme frequency intervals) and the ARX methods adequately represent the system while, the FFT-based spectral estimate yields an unsatisfactory result. This is due to the fact that the input/output data are not windowed for any of the techniques employed. For the spectral approach, this results in corruption due to leakage. It is well known that windowing techniques, such as the use of a Hanning window, can mitigate the corrupting effects of leakage and produce a much smoother response curve for spectral estimation. The drawback of such techniques, however, is that they produce a systematic bias in the estimation, particularly at resonance where there are sharp transitions in the true value of the response function. This can lead in particular to errors in damping and modal mass estimates when the modal model is identified.

Case 2 repeats the first case with the notable exceptions that (1) There is no measurement noise added to the signals; and (2) Anti-aliasing filters are used. The anti-alias filters were designed as low-pass filters with a

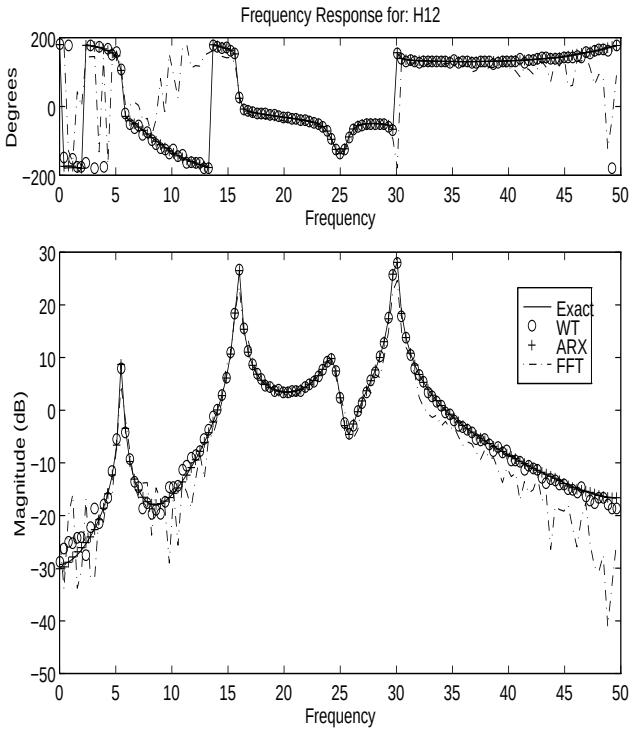

Figure 3: Results For Case 1: H_{12}

corner frequency of $35Hz$ and were applied to the "continuous" ($1000Hz$ sampled) signals before the final signal sampling at $100Hz$. Results for Case 2 are shown in Figure 4. Most notable is the fact that no data for the ARX approach are shown in the figure. Analyzing the results, we found that the causal Markov sequence corresponding to the data pre-filtered with the anti-aliasing filter was found to be unstable. This instability is not entirely unexpected and can probably be traced to the existence of a frequency domain of nonzero measure over which the spectrum of the anti-aliased output vanishes (or nearly so) and, when combined with the additional constraint that the conditions of the comparison have imposed, results in an extreme model over-parameterization. Experience with non-exogenous autoregressive models has shown that the very flat zero created by the anti-aliasing filter leads to poles that are densely populated around the unit circle in the z-plane. Unfortunately, the maximum likelihood estimation of the ARX model is not necessarily stable, which is contrary to the case of non-exogenous AR modeling, and thus some poles are found which reside outside the unit circle.

Note in Figure 4 that both the Wavelet transform estimate and the FFT spectral-based estimate both display a biased trend at points away from the modal resonances. This is, in fact, due to the anti-alias filters used on the time-series data before sampling. In

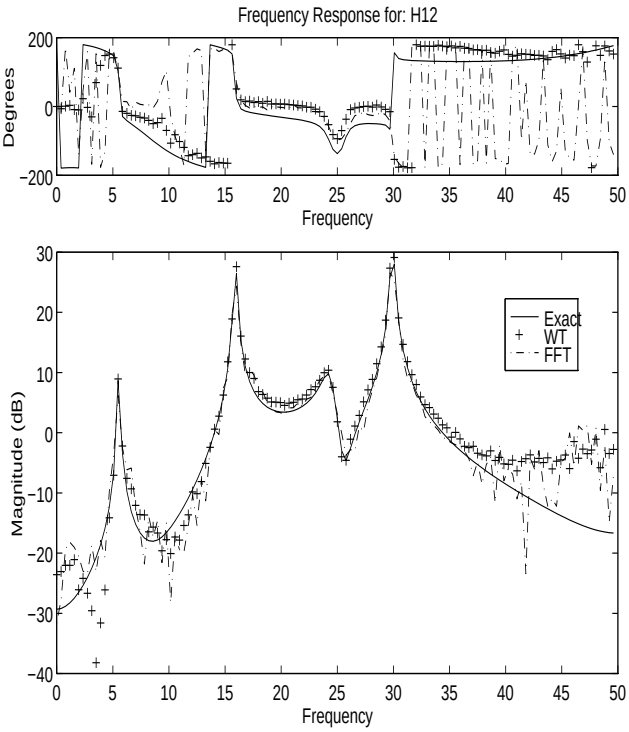

Figure 4: Results For Case 2: H_{12}

the bandwidth below 35 Hz (which was the corner frequency set for the filters), the spectral estimation will tend to converge towards the samples of the continuous FRF which was shown in Figure 1. Above 35 Hz, neither of the estimates will be reliable because the low magnitude of both the input and output renders the estimation indeterminate. Generally speaking, the use of anti-alias filters will bias the estimated FRF towards samples of the continuous FRF within the passband of the filters, while leaving the signals unfiltered will lead to an estimation of the discrete FRF.

6 Concluding Remarks

The subject study was motivated by two key observations: first, current data reduction schemes for extracting modal models from test measurements assume discrete time state-space models underlie the corresponding physical system; and secondly, spectral methods, while exhibiting many well-known strengths, may be deficient in providing input to these procedures in the appropriate form. This latter point has at least one relevant consequence in that it can lead to difficulties in assessing the model order for a given system resulting in an accompanying model that is over-parameterized. The difficulties with over-parameterization include the existence of unstable computational poles, which must be culled, and stable computational poles, which must then be distinguished from poles associated with system modes of vibration—a nontrivial task, at best.

To address these issues, two time series analysis techniques, wavelet transforms and autoregressive with exogenous input, were selected for consideration based on their direct relationships to the discrete time system. A review of the basics for each approach has been presented and the performance of each was examined for two cases of interest. Both methods, under the constraints imposed by the study, performed well for the case of unfiltered data. The ARX approach provided a superb fit, perhaps suggesting that data windowing need not be employed when using it. The Wavelet transform performed equally well for both example cases, while ARX proved a failure. The source of this is the subject of ongoing investigation.

One point that has not been discussed is the computational feasibility of each of the methods. Both suffer in this important aspect relative to FFT-based spectral methods. The wavelet transform approach performs far poorer and additional research on that specific aspect is definitely needed. ARX, and for that matter ARMAX formulations, exhibit computational properties that are less prohibitive and the modeling experience base is far more extensive. Some promise may lie in the fact that incorporating the noise model in the parametric description will render the averaging requirement moot thus lessening the data acquisition load.

A final note: In many ways a one-to-one comparison is made difficult by the artificial constraints that are placed on each method. For example, the over-parameterization for the ARX approach would not have been an issue had the model size not been specified as a condition of the survey. Additional work will focus on how best to characterize the results of each approach, both for the current example set as well as for systems with out-of-band system modes.

References

[1] D. J. Ewins. *Modal Testing: Theory and Practice.* John Wiley and Sons, 1984.

[2] H. Vold, J. Kundrat, G. T. Rocklin, and R. Russell. A Multiple-Input Modal Estimation Algorithm for Mini-Computers. *SAE Transactions* **91/1**, 815–821 (1982).

[3] J. N. Juang and R. S. Pappa. An Eigensystem Realization Algorithm for Modal Parameter Identification and Model Reduction. *Journal of Guidance, Control and Dynamics* **8**, 620–627 (1985).

[4] A. N. Robertson, K. C. Park, and K. F. Alvin. Extraction of Impulse Response Data via Wavelet Transform for Structural System Identification. In

Proceedings of the Design Engineering Technical Conference, DE-Vol. 84-1, Vol 3, Part A, 1995.

[5] I. Daubechies. Orthonormal bases of compactly supported wavelets. *Commun. Pure Appl. Math* **41**, 909–996 (1988).

[6] D. E. Newland. *Random Vibrations, Spectral and Wavelet Analysis*. Longman Scientific and Technical, Essex, England, 1993.

[7] L. Ljung. *System Identification—Theory for the User*. Prentice-Hall, 1987.

[8] W. Gersch and J. Yonemoto. Synthesis of Multivariate Random Vibration Systems: Two-Stage Least Squares AR-MA Model Approach. *Journal of Sound and Vibration* **52**, 553–565 (1977).

[9] J. E. Lee and S. D. Fassois. Suboptimum Maximum Likelihood Estimation of Structural Parameters from Multiple-Excitation Vibration Data. *Journal of Vibration and Acoustics* **114**, 260–271 (1992).

[10] M. P. Mignolet and J. R. Red-Horse. ARMAX Identification of Vibrating Structures: Model and Model Order Estimation. In *Proceedings of the 35th AIAA Structures, Structural Dynamics, and Materials Conference*, 1994.